Structural Rearrangement of Bimetallic Alloy PdAu Nanoparticles within Dendrimer Templates to Yield Core/Shell Configurations†

Marc R. Knecht,‡,|| Michael G. Weir,‡ Anatoly I. Frenkel,*,§ and Richard M. Crooks*,‡

Department of Chemistry and Biochemistry, Texas Materials Institute, Center for Nano- and Molecular Science and Technology, The University of Texas at Austin, 1 University Station, A5300, Austin, Texas 78712-0165, and Department of Physics, Yeshiva University, 245 Lexington Avenue, New York, New York 10016

Received July 5, 2007. Revised Manuscript Received August 6, 2007

Here we present evidence for an oxidation-driven structural conversion of quasi-alloy PdAu dendrimer-encapsulated nanoparticles (DENs) to a Au-core/Pd-shell configuration. The initial quasialloy was prepared by co-complexation of $PdCl_4^{2-}$ and $AuCl_4^-$ within a sixth-generation, poly(amidoamine) dendrimer template followed by chemical reduction. Exposure to air resulted in selective reoxidation of the Pd atoms and subsequent re-reduction led to deposition of a Pd-rich shell on the surface of the remaining Au core. The core/shell nanoparticles were extracted as monolayer-protected clusters (MPCs) from within the dendrimer templates using dodecanethiol. The resulting materials were characterized by UV−vis spectroscopy, transmission electron microscopy, and extended X-ray absorption fine structure (EXAFS) spectroscopy.

Introduction

Here we report a detailed, atomic-level structural study of bimetallic nanoparticles containing an average of 147 atoms synthesized using dendrimer templates.[1] Extended X-ray absorption fine structure (EXAFS) spectroscopy indicates that co-complexation of two metal complexes (K_2PdCl_4 and $HAuCl_4$) with the dendrimer followed by chemical reduction results in formation of zerovalent PdAu quasi-random, dendrimer-encapsulated nanoparticle (DEN) alloys.[1−3] The elemental composition of these DENs reflects the stoichiometry of the Pd and Au complexes used for the synthesis.[4,5] Extraction of the nanoparticles from the dendrimers using alkanethiols results in conversion of the PdAu alloy DENs to monolayer-protected clusters (MPCs)[6−9] having a Au-rich core and a Pd-rich shell (Scheme 1). The results reported here are significant for two reasons. First, PdAu DENs synthesized by co-complexation[1] result in a quasirandom alloy structure, regardless of the relative ratios of the two metals used for the synthesis. Second, EXAFS analysis before and after extraction provides direct evidence for oxidation-driven conversion of a quasirandom alloy nanoparticle to a core/shell structure.

Multimetallic nanoparticles and surfaces often improve the selectivities and rates of metal-catalyzed reactions.[2,5,10,11] For example, the hydrogenation rate of simple olefins is increased in the presence of Pd catalysts containing 20% Au compared to monometallic Pd catalysts.[5,11−14] This increase in activity has been attributed to the electronegativity of the Au atoms, which renders the Pd atoms electron deficient and thus enhances their interaction with the olefinic double bond. Additionally, Pâ rvulescu et al. have shown that PdAu alloy nanoparticles selectively catalyze the hydrogenation of cinnamaldehyde to cinnamyl alcohol over 3-phenyl-1-propanol, which is the preferred product in the presence of monometallic Pd catalysts.[15] Selectivity effects such as this are of particular interest for reactions in which multiple reactive functional groups are present on the same substrate molecule. Finally, Goodman and co-workers have studied the PdAu-catalyzed conversion of potassium acetate to vinyl acetate (VA) and found that the reaction rate was maximized when 0.07

† Part of the "Templated Materials Special Issue".

* To whom correspondence should be addressed. E-mail: crooks@cm.utexas.edu (R.M.C.); anatoly.frenkel@yu.edu (A.I.F.). Phone: (512) 475-8674 (R.M.C.); (212) 340-7827 (A.I.F.).

‡ The University of Texas at Austin.

§ Yeshiva University.

|| Present address: 101 Chemistry-Physics Building, Department of Chemistry, University of Kentucky, Lexington, KY 40506.

(1) Scott, R. W. J.; Wilson, O. M.; Crooks, R. M. *J. Phys. Chem. B* **2005**, *109*, 692–704, and references therein.
(2) Chandler, B. D.; Gilbertson, J. D. *Top. Organomet. Chem.* **2006**, *20*, 97–120.
(3) Crooks, R. M.; Zhao, M.; Sun, L.; Chechik, V.; Yeung, L. K. *Acc. Chem. Res.* **2001**, *34*, 181–190.
(4) Scott, R. W. J.; Sivadinarayana, C.; Wilson, O. M.; Yan, Z.; Goodman, D. W.; Crooks, R. M. *J. Am. Chem. Soc.* **2005**, *127*, 1380–1381.
(5) Scott, R. W. J.; Wilson, O. M.; Oh, S.-K.; Kenik, E. A.; Crooks, R. M. *J. Am. Chem. Soc.* **2004**, *126*, 15583–15591.
(6) Wilson, O. M.; Scott, R. W. J.; Garcia-Martinez, J. C.; Crooks, R. M. *J. Am. Chem. Soc.* **2005**, *127*, 1015–1024.
(7) Wilson, O. M.; Scott, R. W. J.; Garcia-Martinez, J. C.; Crooks, R. M. *Chem. Mater.* **2004**, *16*, 4202–4202.
(8) Garcia-Martinez, J. C.; Scott, R. W. J.; Crooks, R. M. *J. Am. Chem. Soc.* **2003**, *125*, 11190–11191.
(9) Garcia-Martinez, J. C.; Crooks, R. M. *J. Am. Chem. Soc.* **2004**, *126*, 16170–16178.
(10) Scott, R. W. J.; Datye, A. K.; Crooks, R. M. *J. Am. Chem. Soc.* **2003**, *125*, 3708–3709.
(11) Toshima, N.; Yonezawa, T. *New J. Chem.* **1998**, 1179–1201.
(12) Toshima, N.; Harada, M.; Yamazaki, Y.; Asakura, K. *J. Phys. Chem.* **1992**, *96*, 9927–9933.
(13) Mizukoshi, Y.; Fujimoto, T.; Nagata, Y.; Oshima, R.; Maeda, Y. *J. Phys. Chem. B* **2000**, *104*, 6028–6032.
(14) Slocik, J. M.; Naik, R. R. *Adv. Mater.* **2006**, *18*, 1988–1992.

10.1021/cm0717817 CCC: $40.75
Published on Web 10/04/2007

Scheme 1

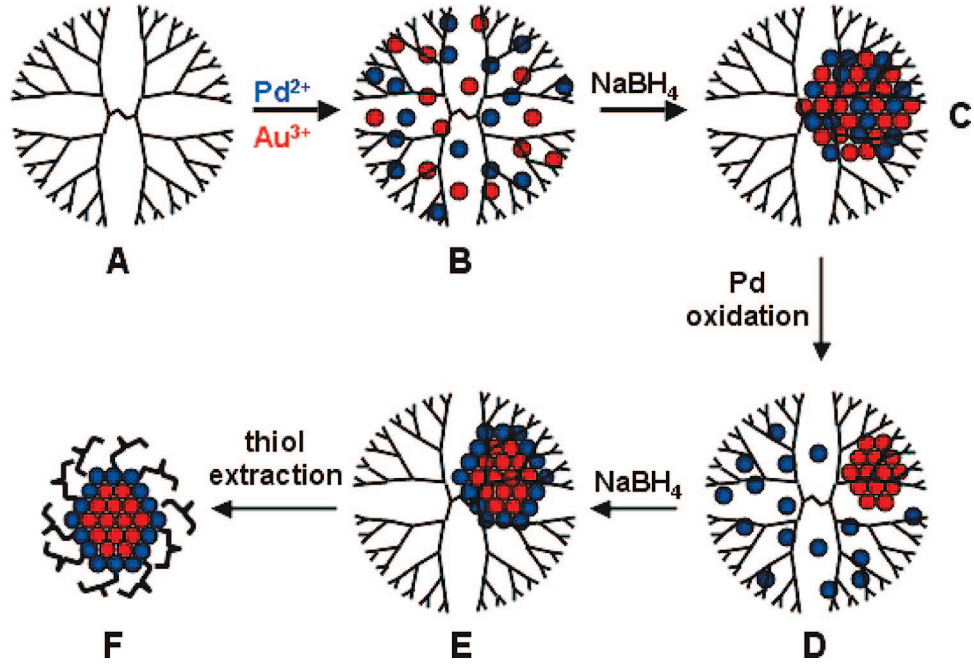

monolayers of Pd were alloyed into a Au(100) surface.[16] There are many other examples demonstrating interesting catalytic properties of PdAu bimetallic surfaces and nanoparticles.[4,5,11–25]

A number of methods have been developed for synthesizing PdAu bimetallic nanomaterials, but one of two general approaches is typically used: simultaneous[4,5,13,15,22,26–30] or sequential[5,20,31,32] reduction of appropriate precursors. For simultaneous reduction, a solution containing Pd^{2+}, Au^{3+}, and a surface passivant is prepared, and reduction is then usually initiated using the polyol method[12,17,20] or by addition of borohydride.[5,15,28,33] Polyol reduction often results in formation of Au-core/Pd-shell nanoparticles[12,13,26,27,29] because of the difference in the reduction potentials of the two metal ions: Au reduces more easily and provides a seed for the reduction of the Pd shell. The sizes of both the core and shell can be controlled by the ratio of Pd:Au used for the synthesis.[13] Conversely, reduction using borohydride derivatives, either in aqueous or organic solvents, typically produces PdAu alloy nanoparticles,[15,28,33] but at least one group has reported formation of a Au-core/Pd-shell structure.[30] The difference between the two reduction methods is likely attributable to differences in relative reducing power of aldehyde groups (polyol synthesis) versus borohydride; the former is a weaker reducing agent than the latter and thus it preferentially initiates the reduction of Au first.

The second approach for preparing bimetallic nanoparticles relies on sequential reduction of two different types of metal ions. In this method, a monometallic core is synthesized first, and then in a second step, the second metal is reduced onto the core surface. This method has been used to synthesize PdAu alloy,[20] Au-core/Pd-shell,[31] and Pd-core/Au-shell[21,32] nanoparticles. Interestingly, the polyol process has been used to sequentially reduce first Pd^{2+} and then Au^{3+} in the presence of a polymer stabilizer at temperatures ranging from 100 to 190 °C.[20] However, because of the elevated temperature, an alloy, rather than a Pd-core/Au-shell structure, resulted from this synthesis.

We have previously reported a template method for synthesizing nanoparticles ranging in size from just a few atoms to about 300.[1,3] This approach has been used to prepare monometallic nanoparticles,[34–46] alloy and core−shell bimetallic nanoparticles,[2,5,6,10,47–49] and semiconducting quantum dots.[50] These DENs are synthesized in two steps.

(15) Pârvulescu, V. I.; Pârvulescu, V.; Endruschat, U.; Filoti, G.; Wagner, F. E.; Kuβel, C.; Richards, R. *Chem.—Eur. J.* **2006**, *12*, 2343–2357.
(16) Chen, M.; Kumar, D.; Yi, C.-W.; Goodman, D. W. *Science* **2005**, *310*, 291–293.
(17) Ferrer, D.; Torres-Castro, A.; Gao, X.; Sepúlveda-Guzmán, S.; Ortiz-Méndez, U.; José-Yacamán, M. *Nano Lett.* **2007**, *7*, 1701–1705.
(18) Lee, A. F.; Baddeley, C. J.; Hardacre, C.; Ormerod, R. M.; Lambert, R. M.; Schmid, G.; West, H. *J. Phys. Chem.* **1995**, *99*, 6096–6102.
(19) Luo, K.; Wei, T.; Yi, C.-W.; Axnanda, S.; Goodman, D. W. *J. Phys. Chem. B* **2005**, *109*, 23517–23522.
(20) Mejfía-Rosales, S. J.; Fernández-Navarro, C.; Pérez-Tijerina, E.; Blom, D. A.; Allard, L. F.; Yacamán, M.-J. *J. Phys. Chem. C* **2007**, *111*, 1256–1260.
(21) Shiraishi, Y.; Ikenaga, D.; Toshima, N. *Aust. J. Chem.* **2003**, *56*, 1025–1029.
(22) Solsona, B. E.; Edwards, J. K.; Landon, P.; Carley, A. F.; Herzing, A.; Kiely, C. J.; Hutchings, G. J. *Chem. Mater.* **2006**, *18*, 2689–2695.
(23) Villa, A.; Champione, C.; Prati, L. *Catal. Lett.* **2007**, *115*, 133–136.
(24) Wang, D.; Villa, A.; Porta, F.; Su, D.; Prati, L. *Chem. Commun.* **2006**, *2006*, 1956–1958.
(25) Wei, T.; Wang, J.; Goodman, D. W. *J. Phys. Chem. C* **2007**, *111*, 8781–8788.
(26) Wu, M.-L.; Chen, D.-H.; Huang, T.-C. *Langmuir* **2001**, *17*, 3877–3883.
(27) Mizukoshi, Y.; Okitsu, K.; Maeda, Y.; Yamamoto, T. A.; Oshima, R.; Nagata, Y. *J. Phys. Chem. B* **1997**, *101*, 7033–7037.
(28) Ge, Z.; Cahill, D. G.; Braun, P. V. *J. Phys. Chem. B* **2004**, *108*, 18870–18875.
(29) Harpeness, R.; Gedanken, A. *Langmuir* **2004**, *20*, 3431–3434.
(30) Nath, S.; Praharaj, S.; Panigrahi, S.; Ghosh, S. K.; Kundu, S.; Basu, S.; Pal, T. *Langmuir* **2005**, *21*, 10405–10408.
(31) Hu, J.-W.; Li, J.-F.; Ren, B.; Wu, D.-Y.; Sun, S.-G.; Tian, Z.-Q. *J. Phys. Chem. C* **2007**, *111*, 1105–1112.
(32) Henglein, A. *J. Phys. Chem. B* **2000**, *104*, 6683–6685.
(33) Bönnemann, H.; Endruschat, U.; Tesche, B.; Ruffínska, A.; Lehmann, C. W.; Wagner, F. E.; Filoti, G.; Pârvulescu, V.; Pârvulescu, V. I. *Eur. J. Inorg. Chem.* **2000**, *2000*, 819–822.

First, metal ions are mixed with the dendrimer template, and in favorable cases, fixed stoichiometries of the metal ions complex with interior functional groups of the dendrimer. Second, a reducing agent is added to this mixture, which results in reduction of the ions within the dendrimer. Subsequently, the atoms agglomerate to yield particles having sizes that reflect the initial metal-ion-to-dendrimer ratio. Variations of this basic approach can lead to multimetallic core/shell or alloy nanoparticles.[2,5,6,10,47–49] Because the dendrimer is porous, the surface of DENs have been found to be catalytically active for homogeneous[2,40,42,45,51,52] and electrocatalytic[43,49,53] reactions. Finally, it is possible to remove the dendrimer and carry out catalytic reactions on the naked nanoparticles.[4,38,47,48,54]

Because of their small size, the characterization of DENs presents some interesting analytical challenges. For simple, monometallic DENs, electron microscopy and UV−vis spectroscopy are useful; however, more sophisticated methods are required to achieve a complete understanding of these materials and particularly of the more complex multimetallic DENs. For example, NMR, EXAFS, and X-ray photoelectron spectroscopy (XPS) have been used to characterize DENs before and after reduction.[43,55–57] Additionally, we have introduced two chemical characterization methods based on selective catalytic reactions[5,11] and selective extraction that complement instrumental methods of analysis.[6–9] These approaches are particularly useful for understanding the structure and composition of multimetallic DENs. For example, in the extraction method, an aqueous DEN solution is mixed with an organic phase containing a hydrophobic ligand that binds preferentially with one of the two metals comprising the particle. If the ligand is selective for a metal present on the surface, then it will adsorb to the nanoparticle surface and in many cases extract the particle from within the dendrimer template.[8,9] This extraction method has been used to speciate nanoparticle mixtures,[7] determine the surface oxidation states of nanoparticles,[6] and distinguish between core and shell metals.[6]

Here we use the DEN extraction method, EXAFS, TEM, and UV−vis spectroscopy to better understand the properties of PdAu bimetallic DENs prepared by co-complexation. DENs consisting of an average of 147 atoms and having five different Pd:Au ratios were synthesized and characterized. EXAFS results indicate that co-complexation of $AuCl_4^-$ and $PdCl_4^{2-}$ with sixth-generation, hydroxyl-terminated poly(amidoamine) (PAMAM) dendrimers (G6-OH) followed by chemical reduction results in formation of zerovalent PdAu DENs having a quasirandom alloy structure regardless of the metal-ion-to-dendrimer ratio used. After extraction of the DENs into hexanes using dodecanethiol ligands, EXAFS indicates that a structural rearrangement occurs that yields MPCs[58] having Au-rich cores and Pd-rich shells (Scheme 1). The structural model for both the DENs and MPCs are supported by TEM and UV−vis results.

Experimental Section

Chemicals. G6-OH PAMAM dendrimers were purchased from Dendritech, Inc. (Midland, MI) as an 11.47 wt% solution in methanol. Prior to use, the methanol was removed under a vacuum at 25 °C, and a 100 μM stock solution was prepared in water. $HAuCl_4 \cdot 3H_2O$, K_2PdCl_4, $NaBH_4$, and dodecanethiol were purchased from Sigma-Aldrich (Milwaukee, WI). Hexanes and methanol were purchased from Fisher Scientific (Pittsburgh, PA), and absolute ethanol was purchased from Aaper Chemical Co. (Shelbyville, KY). Unless otherwise noted, all chemicals were used as received. 18.0 MΩ cm Milli-Q water (Millipore, Bedford, MA) was used throughout.

Characterization. UV−vis absorbance spectra were obtained using a Hewlett-Packard HP8453 spectrometer and quartz cuvettes having an optical path length of 1.00 cm. Depending on the sample, a spectrum of either 2.00 μM G6-OH in water or neat hexanes (no dendrimer) was used as the background. TEM micrographs were obtained using a JEOL-2010F TEM operating at 200 kV. Samples were prepared by dropwise addition of the solution-phase materials onto a 20 nm thick, carbon-coated, 400 mesh Cu grid (EM Sciences, Gibbstown, NJ) followed by solvent evaporation under a vacuum.

EXAFS analysis was conducted at beamline X18B of the National Synchrotron Light Source at the Brookhaven National Laboratory. The nanoparticle samples were dried to a powder and then dispersed onto adhesive tape. The tapes were folded multiple times to ensure homogeneity. The samples were measured in fluorescence mode, using an Ar-filled, five-grid Lytle detector, with the sample positioned at a 45° angle relative to the incident beam. X-ray absorption coefficients were measured from 150 eV below to 1100 and 1250 eV above the Pd K and Au L_3-edges, respectively.

(34) Crespilho, F. N.; Zucolotto, V.; Brett, C. M. A.; Oliveira, O. N.; Nart, F. C. *J. Phys. Chem. B* **2006**, *110*, 17478–17483.
(35) Kim, Y.-G.; Oh, S.-K.; Crooks, R. M. *Chem. Mater.* **2004**, *16*, 167–172.
(36) Knecht, M. R.; Crooks, R. M. *New J. Chem.* **2007**, *31*, 1349–1353.
(37) Knecht, M. R.; Garcia-Martinez, J. C.; Crooks, R. M. *Chem. Mater.* **2006**, *18*, 5039–5044.
(38) Lang, H.; May, R. A.; Iversen, B. L.; Chandler, B. D. *J. Am. Chem. Soc.* **2003**, *125*, 14832–14836.
(39) Mark, S. S.; Bergkvist, M.; Yang, X.; Angert, E. R.; Batt, C. A. *Biomacromolecules* **2006**, *7*, 1884–1897.
(40) Niu, Y.; Yeung, L. K.; Crooks, R. M. *J. Am. Chem. Soc.* **2001**, *123*, 6840–6846.
(41) Scott, R. W. J.; Ye, H.; Henriquez, R. R.; Crooks, R. M. *Chem. Mater.* **2003**, *15*, 3873–3878.
(42) Wilson, O. M.; Knecht, M. R.; Garcia-Martinez, J. C.; Crooks, R. M. *J. Am. Chem. Soc.* **2006**, *128*, 4510–4511.
(43) Ye, H.; Scott, R. W. J.; Crooks, R. M. *Langmuir* **2004**, *20*, 2915–2920.
(44) Zhao, M.; Sun, L.; Crooks, R. M. *J. Am. Chem. Soc.* **1998**, *120*, 4877–4878.
(45) Narayanan, R.; El-Sayed, M. A. *J. Phys. Chem. B* **2004**, *108*, 8572–8580.
(46) Vijayaraghavan, G.; Stevenson, K. J. *Langmuir* **2007**, *23*, 5279–5282.
(47) Hoover, N. N.; Auten, B. J.; Chandler, B. D. *J. Phys. Chem. B* **2006**, *110*, 8606–8612.
(48) Lang, H.; Maldonado, S.; Stevenson, K. J.; Chandler, B. D. *J. Am. Chem. Soc.* **2004**, *126*, 12949–12956.
(49) Ye, H.; Crooks, R. M. *J. Am. Chem. Soc.* **2007**, *129*, 3627–3633.
(50) Lemon, B. I.; Crooks, R. M. *J. Am. Chem. Soc.* **2000**, *122*, 12886–12887.
(51) Zhao, M.; Crooks, R. M. *Angew. Chem., Int. Ed.* **1999**, *38*, 364–366.
(52) Garcia-Martinez, J. C.; Lezutekong, R.; Crooks, R. M. *J. Am. Chem. Soc.* **2005**, *127*, 5097–5103.
(53) Ye, H.; Crooks, R. M. *J. Am. Chem. Soc.* **2005**, *127*, 4930–4934.
(54) Scott, R. W. J.; Wilson, O. M.; Crooks, R. M. *Chem. Mater.* **2004**, *16*, 5682–5688.
(55) Pellechia, P. J.; Gao, J.; Gu, Y.; Ploehn, H. J.; Murphy, C. J. *Inorg. Chem.* **2004**, *43*, 1421–1428.
(56) Ozturk, O.; Black, T. J.; Perrine, K.; Pizzolato, K.; Williams, C. T.; Parsons, F. W.; Ratliff, J. S.; Gao, J.; Murphy, C. J.; Xie, H.; Ploehn, H. J.; Chen, D. A. *Langmuir* **2005**, *21*, 3998–4006.
(57) Alexeev, O. S.; Siani, A.; Lafaye, G.; Williams, C. T.; Ploehn, H. J.; Amiridis, M. D. *J. Phys. Chem. B* **2006**, *110*, 24903–24914.
(58) Templeton, A. C.; Wuelfing, W. P.; Murray, R. W. *Acc. Chem. Res.* **2000**, *33*, 27–36.

The X-ray energy was calibrated prior to examination of each metallic edge by analysis of the corresponding bulk metal foil. EXAFS data were analyzed using the IFEFFIT software package.[59]

Synthesis of PdAu Alloy DENs. Synthesis of G6-OH-($Pd_xAu_{(147-x)}$) (x = 118, 87, 73, 60, 29) DENs generally followed standard literature procedures, but larger volumes were required to provide enough material for EXAFS analysis.[5] For example, the synthesis of G6-OH($Pd_{118}Au_{29}$) was carried out as follows, and except for differences in the metal-ion-to-dendrimer ratio, an identical procedure was used for the other DENs. First, 5.0 mL of a 100 μM G6-OH stock solution was diluted in 237.0 mL of water. Second, 118 equiv of a freshly prepared 10.0 mM K_2PdCl_4 solution in water (5.90 mL) was added to this solution to yield the metal-ion/dendrimer complex denoted as G6-OH(Pd^{2+})$_{118}$. The solution was allowed to stir for 30 min to ensure complete complexation. Third, 29 equiv of a 10.0 mM $HAuCl_4$ solution in water (1.45 mL) was added to the G6-OH(Pd^{2+})$_{118}$ solution. Finally, after the solution was stirred for <1 min, a 10-fold molar excess of a 1.00 M $NaBH_4$ solution, prepared in 0.30 M NaOH, was added to reduce the metal ions within the dendrimer. The final volume of the solution was 250 mL. Reduction was allowed to proceed for at least 15 min prior to analysis. Note that hydroxyl functionalities are known to reduce Au salts to zerovalent metals,[35,60] and therefore, it is important that the $NaBH_4$ reduction be carried out quickly after addition of $HAuCl_4$. DEN samples used for EXAFS were dried by lyopholization (Freezone 12, Labconco Corp.) for ~15 min after initiation of reduction.

Extraction of DENs. Extraction of the PdAu alloy DENs (part C and D of Scheme 1) was carried out 2 h after the initial reduction using a previously described method.[6,8,9] The solutions were exposed to air during this period and during the extraction process, which results in deactivation (oxidation) of the BH_4^- and oxidation of zerovalent Pd within the DENs. Briefly, 125 mL of an aqueous 2.00 μM DEN solution was placed into a separatory funnel. Second, a 100-fold excess of solid $NaBH_4$ was added with respect to the total metal concentration. Next, 125 mL of a 29.4 mM dodecanethiol solution, prepared in hexanes, was layered atop the aqueous solution. The separatory funnel was shaken vertically and vigorously for 5 min, and then allowed to settle for ~10 min. After settling, the organic phase was removed and concentrated on a rotary evaporator to a volume of ~5.00 mL. The resulting MPCs were then precipitated with absolute ethanol to separate them from excess dodecanethiol, and the precipitate was collected by centrifugation. The supernatant was decanted and the MPCs were redissolved in a minimal volume of hexanes. The concentrated solution was then evaporated under a vacuum at 35 °C until dry.

Results and Discussions

Synthesis of PdAu DENs. As discussed in the Experimental Section, the metal-ion/dendrimer precursor was prepared by sequential addition first of $PdCl_4^{2-}$ and then, after 30 min,[41] $AuCl_4^-$, followed by co-reduction. This was necessary because completion of the reaction between $PdCl_4^-$ and the interior tertiary amines of the dendrimer takes ~15 min, but reduction of the metal-ion/dendrimer complex must be carried out immediately after addition of $AuCl_4^-$ (which enters the dendrimer very quickly) because $AuCl_4^-$ can be prematurely reduced by hydroxyl groups present on the dendrimer periphery. If that happens, large Au aggregates

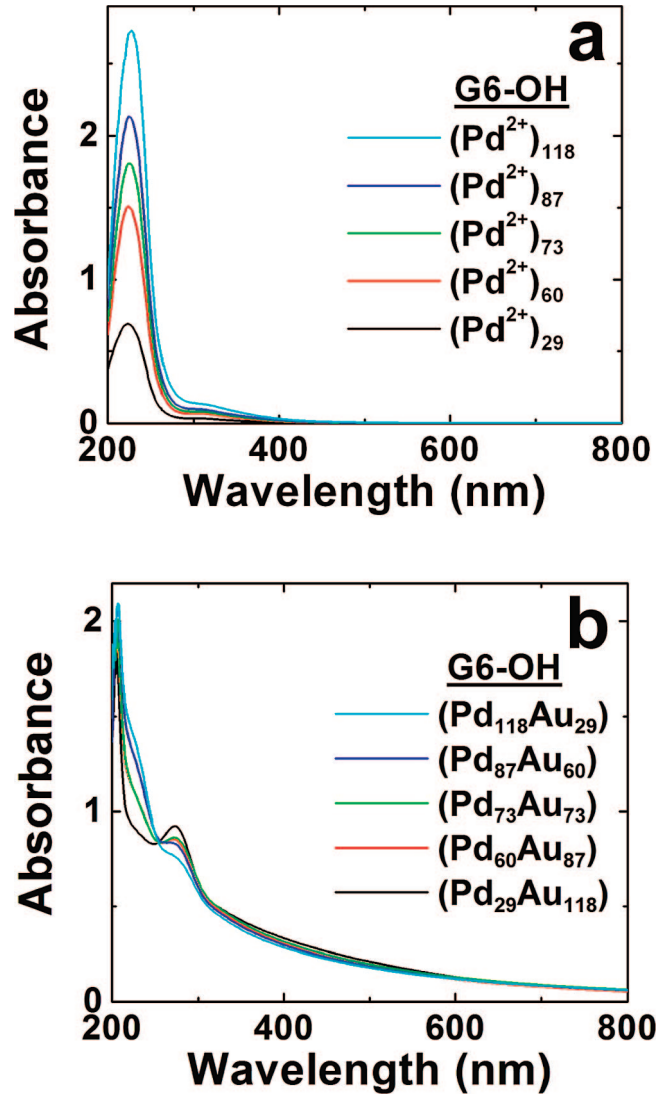

Figure 1. UV−vis spectra of the metal-ion/dendrimer complexes (a) before and (b) after reduction. (a) Only the Pd^{2+} complex is shown, because the dendrimer itself quickly reduces $AuCl_4^-$.

form that are stabilized by multiple dendrimers adsorbed to the metal surface.[35,60,61] Reduction of the metal-ion/dendrimer composite resulted in an immediate color change from pale yellow to brown.

Basic Characterization of PdAu DENs. UV−vis spectroscopy was used to monitor the reaction progress of DEN formation, beginning with Pd-ion complexation and concluding with metal-ion reduction. The UV−vis absorbance spectra of the G6-OH(Pd^{2+})$_n$ (n = 29, 60, 73, 87, and 118) species prior to addition of Au^{3+} are shown in Figure 1a. The prominent band at 221 nm arises from a ligand-to-metal charge transfer (LMCT) between interior amines of the dendrimer and Pd^{2+}.[41] The absorbance of this peak as a function of concentration is linear, indicating an uncomplicated interaction between the Pd complex and the dendrimer. It was not possible to obtain UV−vis spectra of the dendrimer composite with both $PdCl_4^{2-}$ and $AuCl_4^-$, because as mentioned previously, hydroxyl groups on the surface of

(59) Newville, M. *J. Synchrotron Radiat.* **2001**, *8*, 322–324.
(60) Slocik, J. M.; Naik, R.; Stone, M. O.; Wright, D. W. *J. Mater. Chem.* **2005**, *15*, 749–753.
(61) Garcia, M. E.; Baker, L. A.; Crooks, R. M. *Anal. Chem.* **1999**, *71*, 256–258.

the dendrimer reduce the Au complex within a shorter period of time than is required to obtain a reliable spectrum.

UV−vis spectra of the DENs obtained after complexation with $AuCl_4^-$ and subsequent reduction with BH_4^- are shown in Figure 1b. In all cases, the absorbance increases as the wavelength decreases, which is consistent with the presence of nanoscale particles.[62] Additionally, the LMCT band present in Figure 1a at 221 nm is absent, indicating essentially complete reduction of the Pd complex. We have not been able to unambiguously identify the small peak at 285 nm, but as discussed later, it may arise from the dendrimer itself.[63] The erratic behavior at $\lambda < 205$ nm results from imperfect background subtraction of the dendrimer-only solution.

TEM analysis of the particles and their size distribution histograms are provided in Figure 2. Analysis of 100 randomly selected nanoparticles indicate size distributions of 1.4 ± 0.3 nm for G6-OH($Pd_{118}Au_{29}$), 1.5 ± 0.2 nm for G6-OH($Pd_{73}Au_{73}$), and 1.5 ± 0.3 nm for all of the other PdAu DENs. These values are consistent with the calculated diameter of a 147-atom PdAu DEN having a cuboctahedral shape (1.5 nm).[1]

Extraction of PdAu DENs. The method used to extract DENs from within dendrimers has been described in detail previously[6–9] and is briefly discussed in the Experimental Section. Mechanistically, we believe that hydrophobic ligands (dodecanethiol in this case) present in a water/hexanes emulsion penetrate the dendrimer periphery and adsorb to the surface of the encapsulated metal nanoparticle. When the number of ligands bound to the DEN surface exceeds a critical threshold, the particle extracts from the dendrimer as a hydrophobic MPC. In the case of monometallics, the size and optical properties of the MPCs are, within the resolution of the measurements, identical to the parent DENs.[7–9] We have also found that the extraction is dependent on the type of metal present on the surface of the DEN, its oxidation state, and the type of ligand present in the organic phase.[6,7]

The five bimetallic PdAu DENs prepared for this study were extracted using dodecanethiol, and the resulting MPCs were analyzed by UV−vis spectroscopy. Figure 3a provides spectra for the original, aqueous G6-OH($Pd_{118}Au_{29}$) DENs as well as for the aqueous and organic phases after extraction. Spectra for the other four PdAu DENs follow the same trends and are provided in the Supporting Information (Figure S1). Prior to extraction, the spectrum of the water-soluble G6-OH($Pd_{118}Au_{29}$) DENs exhibit an increase in absorbance at lower wavelengths, which is characteristic of small metal nanoparticles,[62] and two peaks. The peak at 285 nm probably arises from the dendrimer, because it is retained in the aqueous phase after extraction (vide infra), but its origin is uncertain at this time. The feature at 205 nm arises from imperfect background subtraction and is actually just the continuation of the rising baseline.[9,35,64]

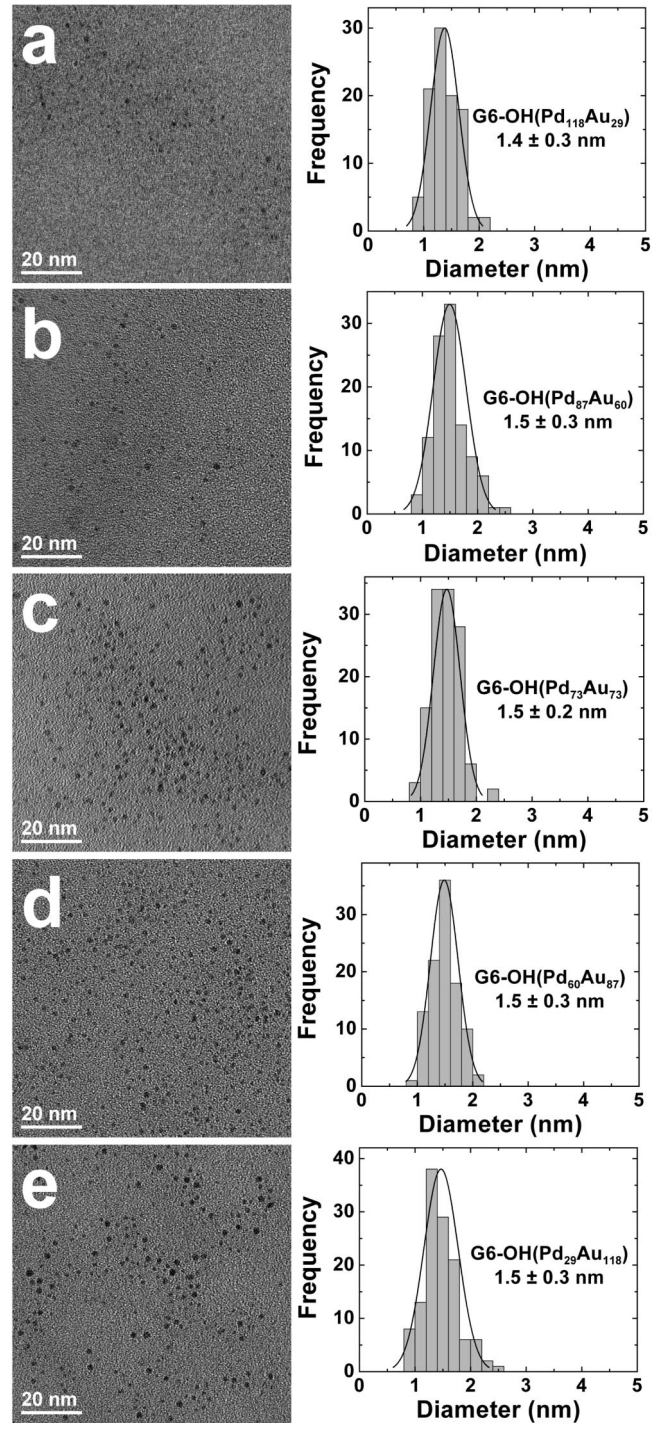

Figure 2. TEM micrographs and particle-size distribution histograms for the indicated compositions of the PdAu DENs.

After extraction, the spectrum of the aqueous layer did not exhibit the rising baseline characteristic of the metal nanoparticles, indicating transfer of the metal nanoparticles to the organic phase. However, as mentioned earlier, the peak at 285 nm is retained, suggesting that it arises from the water-soluble dendrimer[63,65] rather than being associated with the metal nanoparticles. The spectrum of the organic phase tracks the rising baseline of the pre-extraction spectrum, indicating

(62) Creighton, J. A.; Eadon, D. G. *J. Chem. Soc., Faraday Trans.* **1991**, *87*, 3881–3891.
(63) Lee, W. I.; Bae, Y.; Bard, A. J. *J. Am. Chem. Soc.* **2004**, *126*, 8358–8359.
(64) Kim, Y.-G.; Garcia-Martinez, J. C.; Crooks, R. M. *Langmuir* **2005**, *21*, 5485–5491.
(65) Wang, D.; Imae, T.; Miki, M. *J. Colloid Interface Sci.* **2007**, *306*, 222–227.

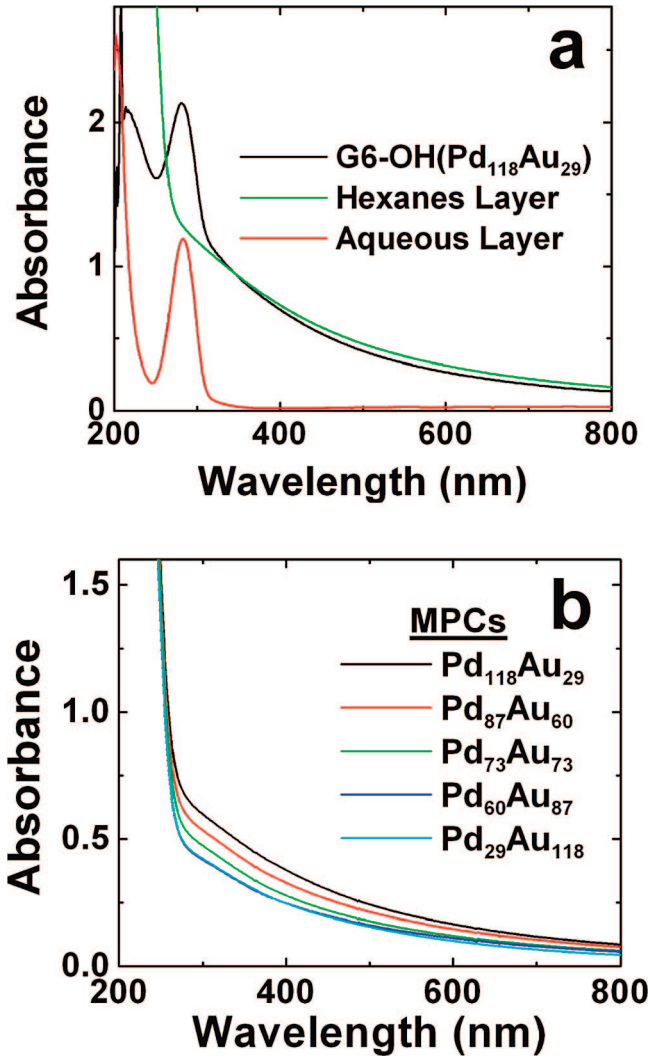

Figure 3. UV−vis spectroscopic analysis of the extraction process. (a) Spectra of the water-soluble G6-OH($Pd_{118}Au_{29}$) DENs prior to extraction, the aqueous layer after extraction with dodecanethiol, and the thiol-passivated $Pd_{118}Au_{29}$ MPCs after extraction. (b) UV−vis spectra of all the extracted PdAu MPCs.

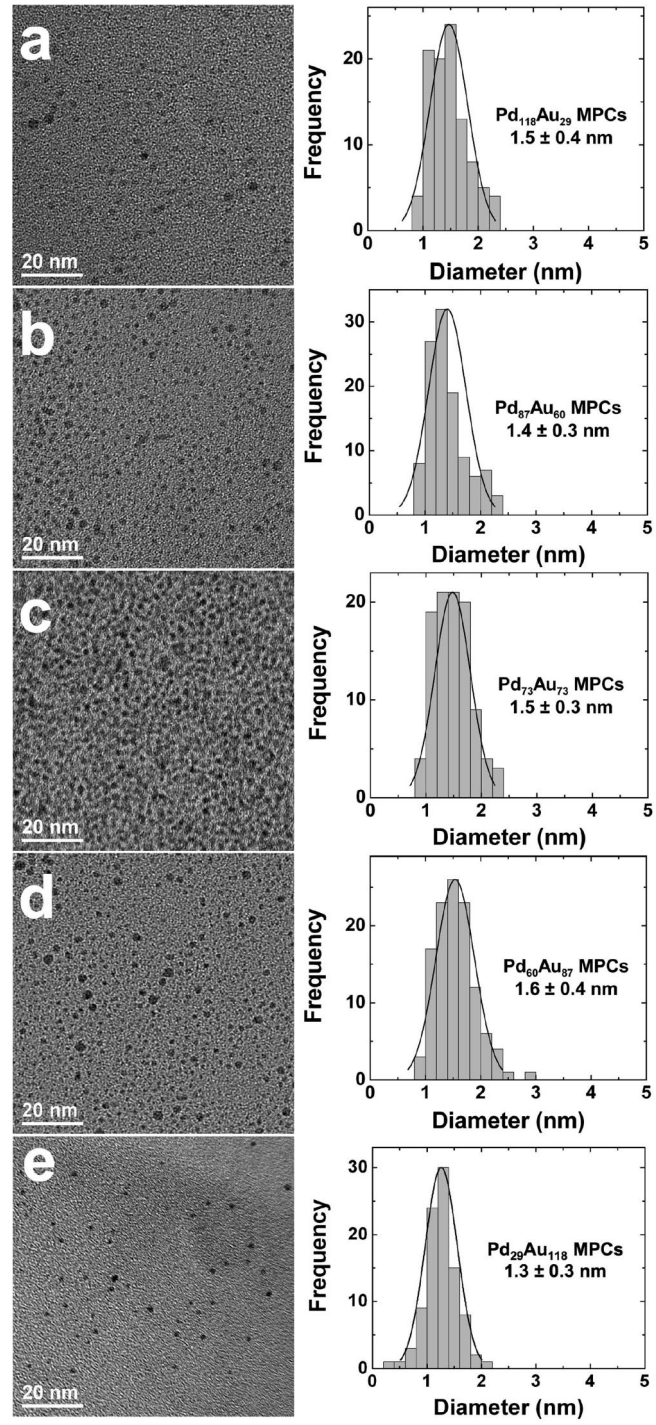

Figure 4. TEM micrographs and particle-size distribution histograms for the PdAu MPCs after extraction with dodecanethiol.

that the metal nanoparticles have been quantitatively transferred as MPCs. The very rapidly rising part of this spectrum ($\lambda \lesssim 250$ nm) arises from absorbance by the solvent (hexanes). Figure 3b shows the UV−vis spectra of all five bimetallic MPCs after extraction into the organic phase. These absorbance spectra are comparable to the corresponding spectra obtained prior to extraction (Figure 1b). This suggests that the DENs are quantitatively extracted into the organic phase as MPCs regardless of their elemental composition. Slight variations in absorbance before and after extraction may arise from incomplete settling of the microemulsion as well as from changes in the nanoparticle structure (vide infra). As in Figure 3a, the rapidly rising baseline in Figure 3b for $\lambda \lesssim 250$ nm arises from absorbance by the solvent.

TEM micrographs and the corresponding size-distribution histograms for the five MPCs are provided in Figure 4. Comparison of these data with those in Figure 2 indicate that extraction does not result in a significant change in average nanoparticle size, although the size distribution does vary slightly.

Principles of Quantitative Analysis of Size, Structure, and Compositional Distributions of Bimetallic Nanoparticles by EXAFS. EXAFS analysis of bimetallic alloys provides accurate information about the short-range order around alloyed elements, A and B, through the measurement of partial coordination numbers n_{AA}, n_{AB}, n_{BA}, and n_{BB}. The analysis should be done concurrently for the data collected

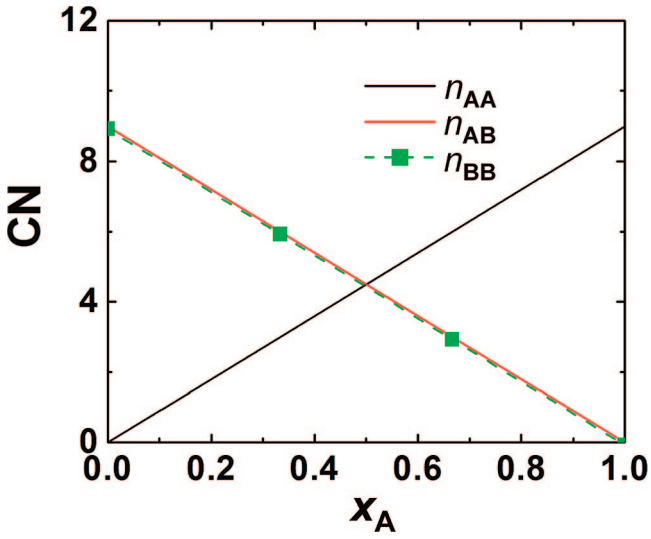

Figure 5. Theoretical partial CNs in random nanoalloys (assuming $n_{MM} = 9$) as a function of composition.

at A and B absorbing atoms, with the following constraints imposed on the heterometallic bonds during the fits.[66]

$$n_{AB} = \frac{x_B}{x_A} n_{BA} \quad (1)$$

$$R_{AB} = R_{BA} \quad (2)$$

$$\sigma^2_{AB} = \sigma^2_{BA} \quad (3)$$

Here, x_A and x_B are elemental compositions. If atoms of type A segregate to the surface of the nanoparticle and the atoms of type B to the core, then $n_{AM} < n_{BM}$, where $n_{AM} = n_{AA} + n_{AB}$ and $n_{BM} = n_{BB} + n_{BA}$, because atoms at the surface have fewer neighbors than those in the core. Random bimetallic alloys have a unique dependence of these coordination numbers (CN) on the alloy concentration. Assume, for simplicity, a bimetallic nanoparticle of a certain size, with a random distribution of A and B atoms, where the following relationships apply.[67]

$$n_{AM} = n_{BM} = n_{MM} \quad (4)$$

$$n_{AA} = n_{BA} = x_A n_{MM} \quad (5)$$

$$n_{BB} = n_{AB} = x_B n_{MM} = (1 - x_A) n_{MM} \quad (6)$$

This analysis indicates that partial CNs should depend linearly on alloy concentration in random nanoalloys, provided that the particle size is the same at all concentrations (Figure 5).

To characterize their short-range order, EXAFS analyses of the bimetallic PdAu nanoparticles was completed for both the DENs and MPCs. For each edge (Pd or Au), up to four consecutive X-ray absorption energy scans were aligned in energy and averaged to minimize statistical noise. The Au and Pd EXAFS data of the same sample were subsequently fit simultaneously in *r*-space using the IFEFFIT software package.[59] CNs, bond lengths, and their disorders, as measured for the Pd−Au bonds from Pd and Au edges, were constrained by eqs 1–3.

EXAFS Characterization of DENs. Figure 6 shows the experimentally obtained Au and Pd EXAFS data for the G6-OH($Pd_{29}Au_{118}$) and G6-OH($Pd_{118}Au_{29}$) DENs, the theoretical fits, trends in CN, and the nearest-neighbor distances. The fitting analysis for other metal ratios is provided in the Supporting Information (Figure S2). Panels e and f in Figure 6 compare the experimentally obtained first nearest-neighbor metal−metal CNs for the DENs. The CNs scale linearly with the Pd concentration (Figure 6e), similar to the ideal random alloy behavior (eq 6 and Figure 5). The difference between the ideal random alloy and the DENs is that CN(Au−M) exceeds CN(Pd−M) over the entire ratio range, as shown in Figure 6f. This result indicates that more Pd atoms reside on the surface of the particles than would be anticipated for a random alloy. This means that the PdAu DENS are quasirandom alloys with a Au-rich core and a Pd-rich shell. Finally, as shown in Figure 6g, the Au−Au, Pd−Au, and Pd−Pd bond distances in the DENs behave as expected for random alloys, because they gradually decrease from the longest values (at low Pd concentrations) to the shortest (at high Pd concentrations), extrapolating to 2.85 Å at $x_{Pd} = 0$ and 2.75 Å at $x_{Pd} = 1$, which agree well with the first nearest neighbor distances in bulk Au (2.87 Å) and Pd (2.75 Å).[68,69] In summary, the EXAFS analysis indicates that the dendrimer-templating method used here results in PdAu DENs having a quasirandom alloy structure. Note that no coordination of the dendrimer through N (or O) ligands was observed, indicating that a significant fraction of the surface metal atoms are freely exposed.

EXAFS Characterization of MPCs. EXAFS analyses of the dodecanethiol-capped PdAu MPCs corresponding to the DENs represented in Figure 6 are provided in Figure 7. The fitting analysis for other concentrations is presented in the Supporting Information (Figure S3). The results indicate a structural rearrangement of the metallic architecture in response to the extraction process. Similar to the DEN parents, the number of Pd−Pd coordinations increases with increasing numbers of Pd atoms per MPC (Figure 7e); however, at the lowest concentration of Pd atoms, no Pd−Pd coordinations are observed. The Au−Au CN was found to be ~7.5 for all the MPCs except for the most Pd-rich nanoparticle ($Pd_{118}Au_{29}$, $x_{Pd} = 0.8$), which exhibited a Au−Au CN of 4.30 ± 1.8. For the Pd−Au coordinations, a nonlinear decrease was observed for the particles as the concentration of Pd increased. These EXAFS results are markedly different from those obtained for the DENs, which indicates a change in the structure of the nanoparticles after extraction.

The CNs for the dodecanethiol ligands present on the surface of the MPCs provides additional clues as to the structure of these materials. As shown in Figure 7e, S interactions were observed only for Pd except for MPCs having the highest ratio of Au ($Pd_{29}Au_{118}$, $x_{Pd} = 0.2$). The Pd−S CN was found to be ~3 for all values of x_{Pd}, which

(66) Nashner, M. S.; Frenkel, A. I.; Adler, D. L.; Shapley, J. R.; Nuzzo, R. G. *J. Am. Chem. Soc.* **1997**, *119*, 7760–7771.
(67) Frenkel, A. I. *Z. Kristallogr.* **2007**,accepted.
(68) Sun, Y.; Frenkel, A. I.; Isseroff, R.; Shonbrun, C.; Forman, M.; Shin, K.; Koga, T.; White, H.; Zhang, L.; Zhu, Y.; Rafailovich, M. H.; Sokolov, J. C. *Langmuir* **2006**, *22*, 807–816.
(69) Frenkel, A. I.; Nemzer, S.; Pister, I.; Soussan, L.; Harris, T.; Sun, Y.; Rafailovich, M. H. *J. Chem. Phys.* **2005**, *123*, 184701.

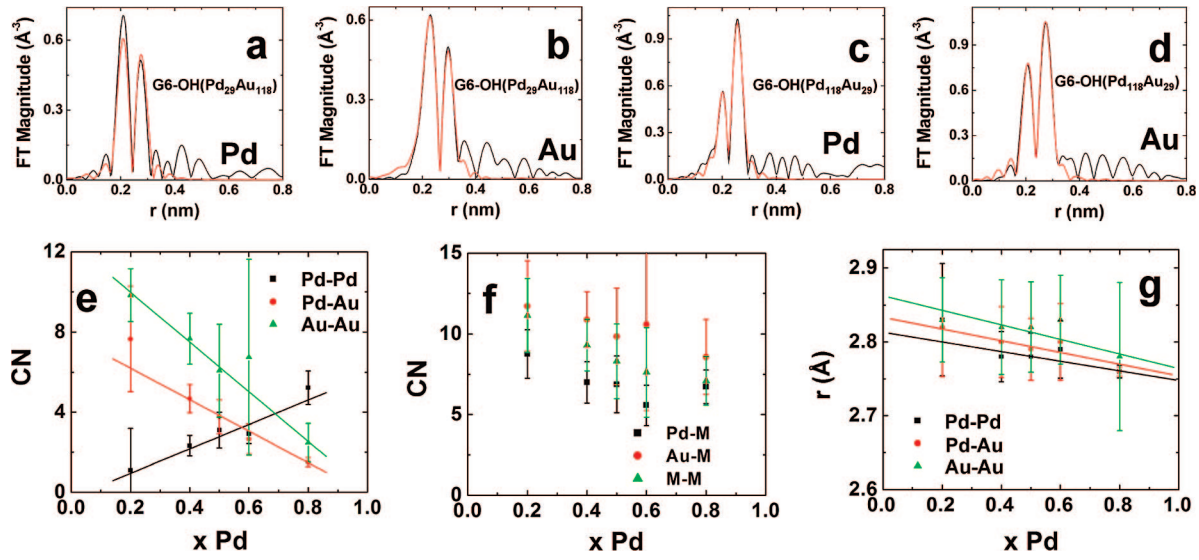

Figure 6. EXAFS data and the corresponding fitting analyses for the Pd K-edge and Au L_3-edge EXAFS for (a, b) G6-OH($Pd_{29}Au_{118}$) and (c, d) G6-OH($Pd_{118}Au_{29}$) DENs. In parts a−d, the data are plotted in black and the simulated fits are plotted in red. (e) Experimentally obtained partial CNs for Pd−Pd, Pd−Au, and Au−Au DENs. (f) Pd−M, Au−M, and M−M CNs as a function of Pd composition. (g) Metal−metal bond lengths for the PdAu DENs.

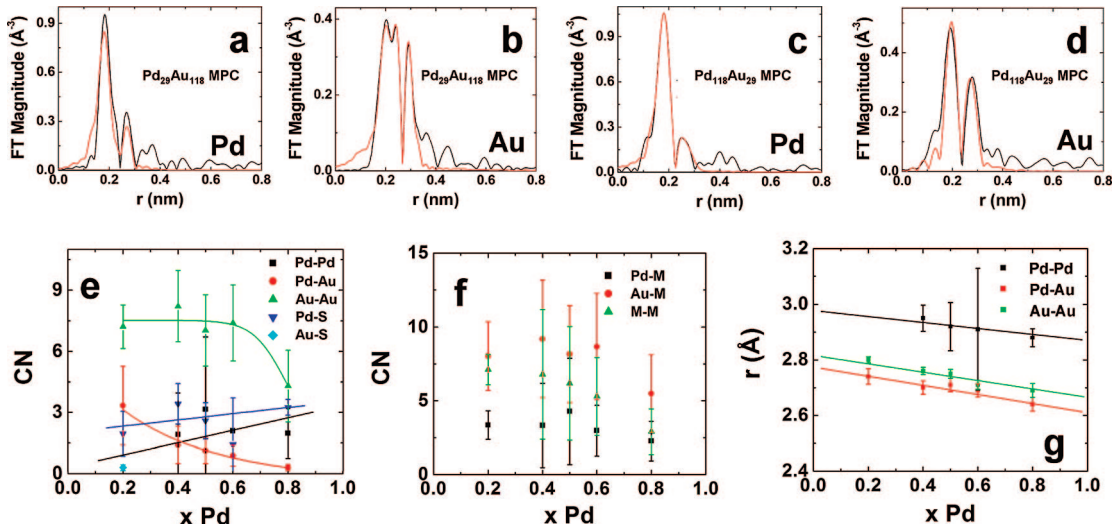

Figure 7. EXAFS data and the corresponding fitting analyses for the Pd K-edge and Au L_3-edge EXAFS for (a, b) $Pd_{29}Au_{118}$ and (c, d) $Pd_{118}Au_{29}$ MPCs. In parts a−d, the data are plotted in black and the simulated fits are plotted in red. (e) Experimentally obtained partial CNs for Pd−Pd, Pd−Au, and Au−Au MPCs. (f) Pd−M, Au−M, and M−M CNs as a function of Pd composition. (g) Metal−metal bond lengths for the PdAu MPCs.

is larger than expected for nanoparticles of this size.[70] If we assume that the surface concentration of alkylthiols on Pd nanoparticles is the same as has been found on Au MPCs, then a Pd−S CN of ~0.5 is anticipated.[58,70,71] Additionally, the total metal−metal CN (M−M, Figure 7f) ranges from approximately 3 ($x_{Pd} = 0.8$) to 7 ($x_{Pd} = 0.2$), which is smaller than the value of 8.98 predicted for cuboctahedral particles of this size.[72] These two observations are consistent with a model that invokes two different Pd−S interaction motifs. Specifically, one model involves dodecanethiol bound to surface Pd atoms of the MPCs, and the other involves dodecanethiol coordinated to single Pd ions (or very small clusters of Pd atoms or ions). Indeed, such Pd−S complexes have previously been observed for Pd MPCs[68,73] resulting in larger than expected Pd−S CNs and smaller than expected Pd−Pd CNs.[68]

Correlation of the Proposed Model and the Experimental Results. The MPC EXAFS results are consistent with oxidatively driven de-alloying of the PdAu alloy DENs as shown in Scheme 1. In this model, some or all of the Pd atoms within the DENs oxidize in the presence of air. This results in formation of more noble Au-only (or mostly) nanoparticles and reconstitution of the Pd^{2+}/dendrimer complex (part D in Scheme 1). During extraction, however, a large excess of reducing agent is added, which results in deposition of Pd atoms onto the surface of the Au core (part E in Scheme 1). This is followed by extraction as an MPC (part F in Scheme 1).

(70) Knecht, M. R.; Jeon, Y. J.; Weir, M. G.; Petkov, V.; Frenkel, A. I.; Crooks, R. M., in preparation.
(71) Sellers, H.; Ulman, A.; Schnidman, Y.; Eilers, J. E. *J. Am. Chem. Soc.* **1993**, *115*, 9389–9401.
(72) Glasner, D.; Frenkel, A. I. *XAFS13 Conf. Proc.* **2007**, *882*, 746–748.
(73) Zamborini, F. P.; Gross, S. M.; Murray, R. W. *Langmuir* **2001**, *17*, 481–488.

The proposed model is supported by the following findings. First, Pd−M CNs are much smaller (typically by a factor of 2) than Au−M CNs (Figure 7f), indicating that segregation of Pd on the surface of the MPCs is more pronounced than for the PdAu DENs (Figure 6f). This Pd-rich structure is also consistent with our finding that Au−S interactions are observed only at the lowest value of x_{Pd}, whereas Pd−S interactions are observed at all values of x_{Pd}. Note, however, that the latter observation is complicated by the likely presence of Pd−thiol complexes. Eventually, as the number of Au atoms per particle increases ($x_{Pd} = 0.2$), a sufficient number of them are present on the surface that Au−S interactions are observed.

Figure 7g is of particular interest, because it independently confirms surface segregation of Pd atoms. In other examples of binary alloys consisting of two species A and B with different nearest neighbor distances *a* and *b*, respectively, it has been found by EXAFS that the bond lengths at all concentrations are located between *a* and *b*.[74–77] For the PdAu DENs, we found this rule to hold (Figure 6g), but it does not hold for the PdAu MPCs. Specifically, the data in Figure 7g show that the Pd−Pd bond is distinctly longer than either the Au−Au or Pd−Au bonds at all Pd:Au ratios as well as in bulk Au (2.87 Å). This anomalous behavior is likely the result of particle surface relaxation, wherein Pd atoms shift away from the normal fcc sites, resulting in longer Pd−Pd bonds. Such displacements must be accompanied by enhanced disorder, which is represented by σ^2. Indeed, σ^2 values for the Pd−Pd bonds are much larger for the MPCs compared to the DENs (see the Supporting Information, Table S1).

Figure 8 provides additional support for the model shown in Scheme 1. Specifically, Figure 8a demonstrates the effects of exposure of G6-OH($Pd_{118}Au_{29}$) DENs to air after reduction. Prior to reduction, the LMCT band at 221 nm for the Pd^{2+}/amine interaction is evident. After $AuCl_4^-$ addition and BH_4^- reduction, the LMCT band disappears and a spectrum reminiscent to that shown in Figure 1b is obtained demonstrating nearly complete Pd-ion reduction. After exposure of the reduced DEN sample to air for ~2 h, a peak at 221 nm is observed that is consistent with Pd atom oxidation and reconstitution to form the Pd^{2+}/dendrimer composite with the reduced Au nanoparticles remaining after oxidation. After introduction of additional BH_4^- for the extraction process, the peak at 221 nm decreases in intensity, indicating reduction of Pd^{2+}, which can deposit along the surface of the nascent Au DENs. The LMCT band does not completely disappear after the secondary reduction, suggesting that not all of the oxidized Pd^{2+} ions have been reduced immediately prior to extraction. Note that the peak at 285 nm, which we correlated to the dendrimer earlier, is present after exposure of the DEN solution to air for 2.00 h. This might suggest that this peak arises from oxidation of the dendrimer.

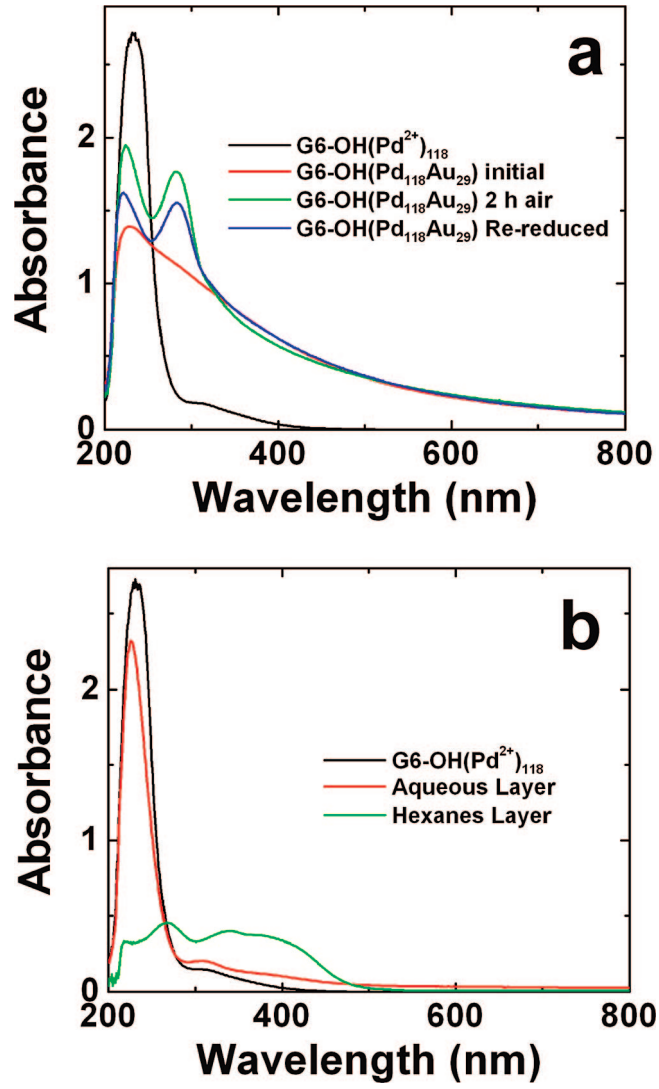

Figure 8. UV−vis spectra demonstrating air oxidation of Pd DENs and dodecanethiol-induced extraction of Pd ions from the dendrimer interior. (a) Spectra of the G6-OH(Pd^{2+})$_{118}$ complex prior to reduction, after reduction with BH_4^-, after exposure to air for 2 h, and after a second reduction. (b) Spectra of G6-OH(Pd^{2+})$_{118}$ before and after extraction with dodecanethiol but in the absence of a reducing agent. A 100-fold stoichiometric excess (relative to Pd^{2+}) of KCl was added to the solution to maintain approximately the same ionic strength used for the extraction of DENs. Spectra of both the aqueous and organic layers are shown.

Because the extraction process is completed with PdAu DEN species that are not fully reduced, it is possible that the unreduced Pd^{2+} can be extracted as well. This effect would give rise to the experimentally observed decrease in the M−M CN in the extracted MPCs (Figure 7f). To confirm this hypothesis, we carried out a control experiment in which the steps required for extraction were carried out on the G6-OH(Pd^{2+})$_{118}$ complex prior to reduction (Figure 8b). Before addition of dodecanethiol the typical LMCT band at 221 nm was observed. After addition of a solution of hexanes containing dodecanethiol, a slight decrease in the absorbance at 221 nm is observed in the aqueous phase and a slight increase is observed in the organic phase. These results suggest that Pd^{2+}/thiol complexes extract into the organic phase, and this finding is consistent with both the large Pd−S CN and the small M−M CN obtained for the PdAu MPCs.

(74) Frenkel, A. I.; Stern, E. A.; Voronel, A.; Qian, M.; Newville, M. *Phys. Rev. Lett.* **1993**, *71*, 3485–3488.
(75) Frenkel, A. I.; Stern, E. A.; Voronel, A.; Heald, S. *Solid State Commun.* **1996**, *99*, 67–71.
(76) Boyce, J. B.; Mikkelsen, J. C. *Phys. Rev. B* **1085**, *31*, 6903–6905.
(77) Frenkel, A. I.; Machavariani, V. S.; Rubshtein, A.; Rosenberg, Y.; Voronel, A.; Stern, E. A. *Phys. Rev. B* **2000**, *62*, 9364–9371.

Summary and Conclusions

We prepared bimetallic PdAu DENs by co-complexing metal ions with dendrimers and then reducing. The resulting materials are nearly monodisperse in size. EXAFS data indicate that the PdAu DENs are quasi-random alloys regardless of their relative elemental composition. Dodecanethiol extraction of the materials into hexanes results in the formation of Au-core/Pd-shell MPCs. In addition, we postulate a model in which Pd/thiol complexes are also extracted from the dendrimers to account for the both the large Pd−S CN and the small M−M CN.

The structural rearrangement that occurs upon extraction (Scheme 1) is likely due to Pd oxidation and re-reduction during the extraction. This change in structure is unusual and likely the result of the oxidized Pd atoms being sequestered within the dendrimer near the Au monometallic core. We also considered a model in which the structural rearrangement was driven by the thiol ligand (rather than metal oxidation). However, because the thiol binding strength to Au is stronger than to Pd, we anticipated that a ligand-driven structural change would result in a Pd-core/Au-shell configuration.[78] Accordingly, we do not consider this mechanism to be likely.

Acknowledgment. We gratefully acknowledge the Robert A. Welch Foundation, the National Science Foundation (Grant 0531030), and the U.S. Department of Energy (DOE-BES Catalysis Science, Grants DE-FG02-03ER15471 and DE-FG02-03ER15476) for financial support of this work. We further acknowledge the Robert A. Welch Foundation and SPRING for support of the facilities used to carry out this project. Beamline X18B is supported by the NSLS, through the Divisions of Materials and Chemical Sciences of the DOE, and the Synchrotron Catalysis Consortium (U.S. DOE Grant DE-FG02-05ER15688).

Supporting Information Available: UV−vis spectra obtained before and after extraction, EXAFS data and fitting analysis for DENs and MPCs, and a table of σ^2 values (PDF). This material is available free of charge via the Internet at http://pubs.acs.org.

CM0717817

(78) CRC Handbook of Chemistry and Physics, 87th ed.; Lide, D. R., Ed.;Taylor and Francis: New York, 2006.